Resonant excitation of surface plasmons in one-dimensional metallic grating structures at microwave frequencies

S Sena Akarca-Biyikli, Irfan Bulu and Ekmel Ozbay

Department of Physics, Bilkent University, Bilkent, Ankara 06800, Turkey

E-mail: sbiyikli@fen.bilkent.edu.tr

Abstract
Grating-coupling phenomena between surface plasmons and electromagnetic waves were studied in the microwave spectrum using metallic gratings. Transmission measurements were carried out to observe the transmitted radiation around the surface plasmon resonance frequencies. Grating structures with subwavelength apertures were designed for transmission experiments. Measurements were made in the microwave spectrum of 10–37.5 GHz, corresponding to a wavelength region of 8–30 mm. The Al samples had a grating periodicity of 16 mm. A 2 mm wide subwavelength slit was opened for transmission samples. Samples with one/double-sided gratings displayed remarkably enhanced transmission and directivity with respect to the reference sample without gratings. The experimental results agreed well with theoretical simulations. $\sim$50% transmission at 20.7 mm, $\sim$25-fold enhancement, and $\pm4°$ angular divergence were achieved with a $\sim\lambda/10$ aperture.

(Some figures in this article are in colour only in the electronic version)

1. Introduction

Surface plasmons (SPs) can be described as oscillations of the surface electron density on metallic surfaces. These charge density waves can be characterized by intense electromagnetic fields confined to the surface. SP modes have longer wavevectors than light waves of the same energy. Therefore, SP waves are non-radiative on smooth metallic surfaces and cannot propagate in non-metallic media [1]. One way to excite SPs is the grating coupling technique, in which the incident radiation is coupled to SPs using periodic surface corrugation [2]. In 1998, Ebbesen *et al* demonstrated extraordinary optical transmission (EOT) through subwavelength hole array structures [3]. Afterwards, many theoretical and experimental studies on EOT through subwavelength apertures (holes or slits) proved that this phenomenon was due to resonant excitation of SPs. 1D

[4–12] and 2D [13–19] periodic surface corrugations were implemented in these studies. The optical beaming property of subwavelength apertures in metallic grating structures was reported [9]. In another study, enhanced transmission through subwavelength hole arrays was shown at THz frequencies [20].

Similar studies were carried out at microwave frequencies by Hibbins *et al* recently. Using grating structures, they have demonstrated the coupling of microwave radiation to SPs by reflection measurements [21, 22]. They have also presented microwave transmission enhancement through a subwavelength slit without a grating [23]. Very recently, Lockyear *et al* have reported enhanced transmission at microwave frequencies through a circular subwavelength aperture surrounded by periodic concentric grooves [24]. To our knowledge, enhanced microwave transmission in 1D grating structures with subwavelength slit aperture has not been reported previously. In this work, we experimentally
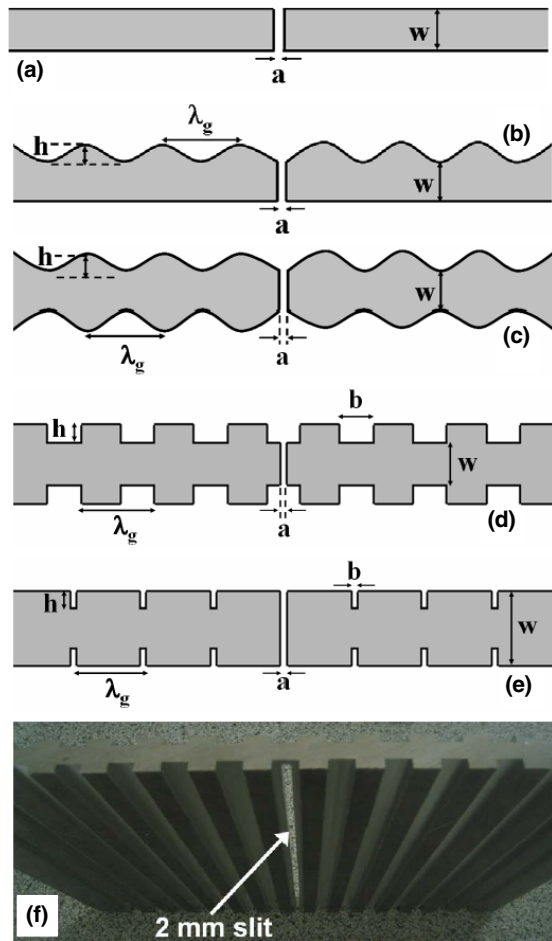
Figure 1. Schematic illustrations of the transmission samples. (a) Gratingless reference sample with thickness $w = 8$ mm and slit width $a = 2$ mm. (b) One-sided sinusoidal grating sample with grating period (λ_g) = 16 mm, groove depth (h) = 4 mm, $w = 8$ mm and $a = 2$ mm. (c) Double-sided sinusoidal grating sample with $\lambda_g = 16$ mm, $a = 2$ mm, $w = 8$ mm, and $h = 4$ mm. (d) Double-sided symmetric rectangular sample with $\lambda_g = 16$ mm, $a = 2$ mm, $b = 8$ mm, $w = 8$ mm, and $h = 4$ mm. (e) Double-sided asymmetric rectangular sample with $\lambda_g = 16$ mm, $a = 2$ mm, $b = 2$ mm, $w = 16$ mm, and $h = 4$ mm. (f) Photograph of the metallic double-sided symmetric rectangular grating sample.

and theoretically demonstrate transmission enhancement and beaming of microwave radiation through a subwavelength slit surrounded by periodic gratings.

2. Experimental details

Five samples were designed for microwave transmission measurements. All five samples had 2 mm wide slit apertures centred on the metallic structure. Schematic illustrations of the transmission samples are shown in figure 1. The gratingless sample with thickness $w = 8$ mm was our reference sample for transmission measurements (figure 1(a)). The one-sided sinusoidal grating sample (figure 1(b)) was designed to analyse the impact of the illumination scheme (front/back illuminated). The grating period was 16 mm, and the groove depth was 4 mm. We have designed three double-sided grating samples with different geometries (figures 1(c)–(e)): sinusoidal, symmetric rectangular, and asymmetric rectangular. These samples had
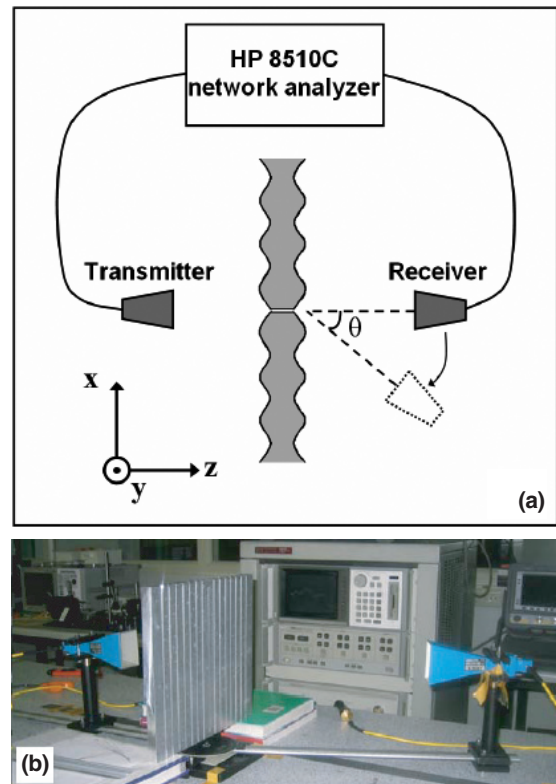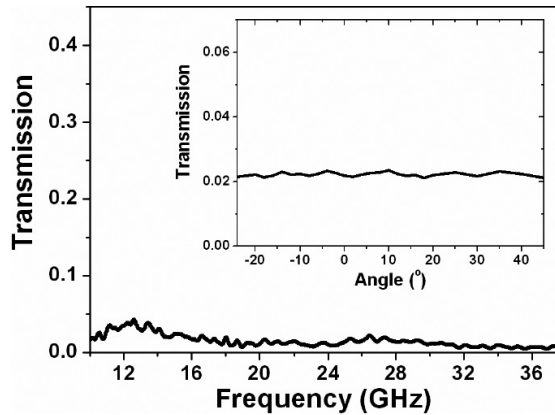
Figure 2. (a) Schematic diagram of transmission measurement set-up. (b) Photograph of transmission measurement set-up with asymmetric rectangular grating sample.

the same grating period (16 mm) and groove depth (4 mm). The groove width for the asymmetric rectangular grating sample was $b = 2$ mm. Since the slit coincides with the groove in this sample, the thickness of the asymmetric rectangular sample was taken as 16 mm instead of 8 mm (figure 1(e)). To determine the enhancement factor of this sample, a reference sample with thickness of 16 mm was utilized. Figure 1(f) shows a photograph of the metallic Al (double-sided) symmetric rectangular grating sample. The samples were fabricated using a CNC machining set-up with 0.1 mm process resolution. All samples were made of metallic aluminium (Al).

Our experimental set-up consists of a 50 GHz HP-8510C network analyser and two microwave horn antennas. The horn antennas were placed on rotating arms for angular measurements. The measurements were made in two frequency ranges: 10–20 and 20–37.5 GHz. Antennas with horn sizes of 42×60 and 29×42 mm^2 were utilized for these frequency ranges, respectively. A schematic diagram of the transmission set-up is presented in figure 2(a).

For transmission measurements, both transmitter and receiver antennas were arranged to be in TM mode (p–p configuration), so that electric field was perpendicular to the groove direction. Excitation of SPs was not possible in the s–s configuration, as grating coupling of SPs cannot occur when the electric field is parallel to the surface corrugation (along the y-axis). The azimuthal angle of the sample was held constant at $\phi = 0°$, and the transmission spectrum at different polar angles θ was recorded. The transmitter antenna was put 15 cm away from the sample. Input radiation was normally incident upon the sample. The receiver antenna was 30 cm away from

Figure 3. Measured transmission spectrum of the reference sample. (Inset) Transmission intensity at 15 GHz, as a function of reception angle.

the sample's back face and it was connected to a rotating arm to measure the angular (θ) dependence of the far-field radiation (figure 2(a)). A photograph of the transmission measurement set-up with the asymmetric rectangular grating sample under test is shown in figure 2(b).

Theoretical calculations were done using finite-difference-time-domain (FDTD) method-based simulations. We modelled our structure by using the Drude dispersion model, i.e., $\varepsilon(\omega) = 1 - \frac{\omega_p^2}{\omega(\omega - i\omega_\tau)}$, where $\omega_p = 3570$ THz is the plasma frequency, and $\omega_\tau = 19.4$ THz is the absorption coefficient for aluminium [25].

3. Results and discussion

Before the transmission measurements of fabricated samples, calibration was done. The transmitted power was recorded while no sample was placed between the antennas. Transmission measurements were made in the 10–37.5 GHz frequency range using both sets of antennas. This frequency spectrum corresponds to the 8–30 mm wavelength spectrum. Since the slit apertures were 2 mm wide, the subwavelength condition was satisfied over this spectrum ($\lambda/15 < a < \lambda/4$). First, the reference (gratingless) sample was measured. Figure 3 shows the measured absolute transmission spectrum of the reference sample. The transmitted power through the slit aperture was weak: only ~1–4% of the input power was transmitted. The transmitted radiation was fully diffracted at all wavelengths, as expected for conventional planary subwavelength apertures. The inset figure shows the transmission intensity versus reception angle θ, measured at 15 GHz ($\lambda = 20$ mm $= 10a$). The transmission intensity was almost the same from $\theta = -30°$ to $45°$, fluctuating around 2%. No directivity was observed in the transmitted radiation. Hence, the microwave transmission through a subwavelength slit aperture was low and fully diffracted.
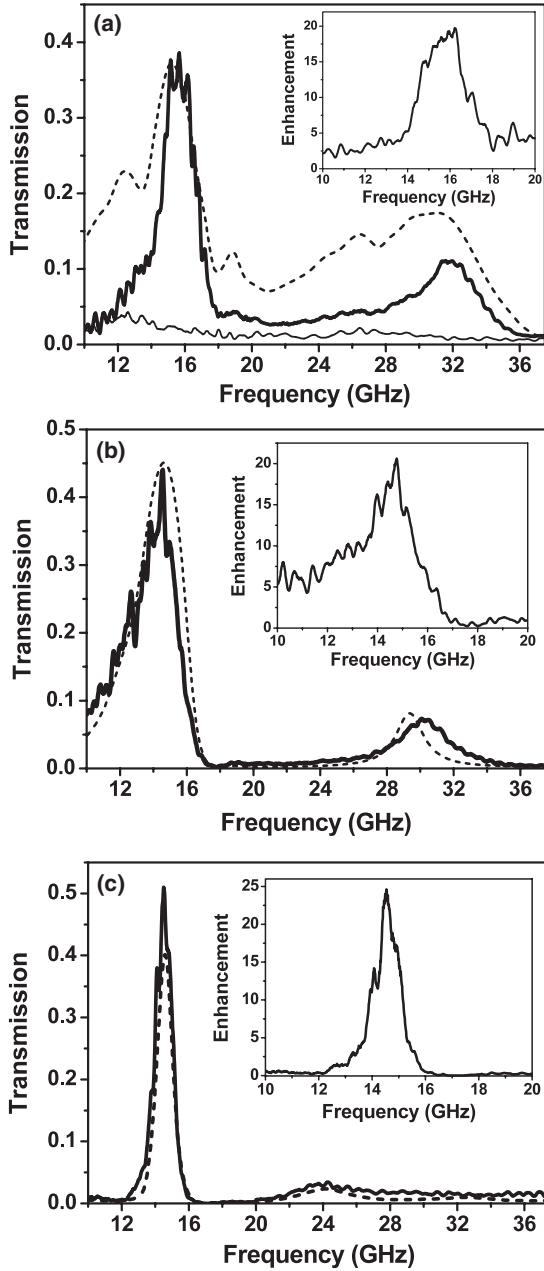
Figures 4(a) and (b) show the front- and back-illuminated spectral transmission curves of the one-sided sinusoidal grating sample, respectively. In the front-illuminated scheme, the grating side of the sample was facing the transmitter. A transmission peak was observed around 16 GHz for both samples. Peak transmission of ~8% at 15.1 GHz and ~10% at 16.1 GHz was measured for front- and back-illuminated
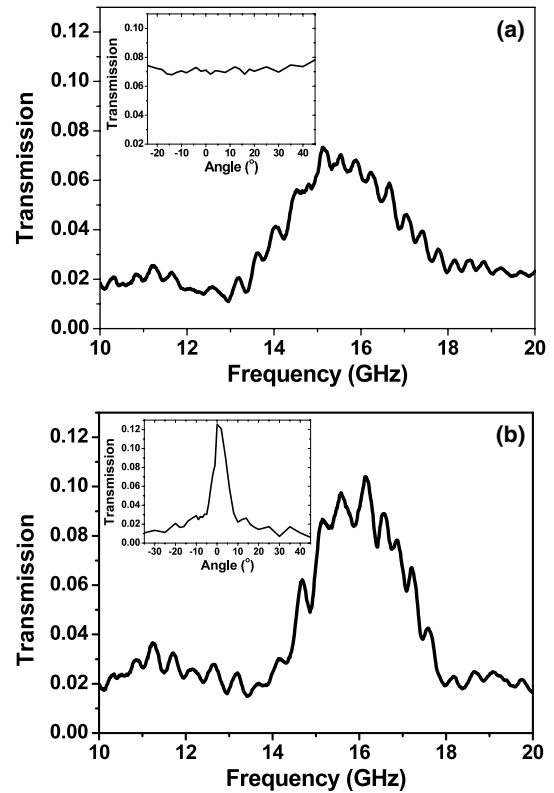
Figure 4. Measured transmission spectra for (a) front-illuminated and (b) back-illuminated one-sided grating samples. Angular dependences of transmission intensities at peak frequencies are shown in the inset figures.

schemes, respectively. When compared with the reference sample, these values correspond to an enhancement factor of ~4 and ~6 at the respective resonance frequencies. The angular dependences of peak transmission intensities are shown in the inset figures. No directivity (beaming) was observed in the front-illuminated sample. The output power radiated uniformly in all directions, similar to the behaviour of the reference sample. When the same sample was illuminated from the planar (back) side, a strong angular dependence was observed. The intensity versus polar angle plot implied that the transmitted light emerged in the shape of a well defined beam with an observed full width at half maximum (FWHM) of 8°. These results show that the grating on the front (illuminated) face enhances the transmission by improving the coupling-in efficiency and the grating on the back (non-illuminated) face gives directionality to the beam. The results from one-sided grating structures tell us that transmission enhancement with higher peaks should be available with double-sided grating structures.
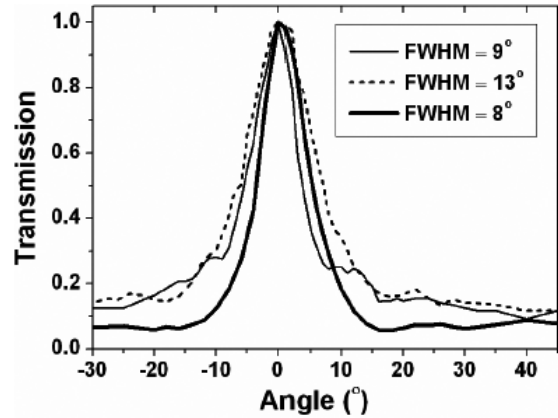
The measurement and simulation results obtained with three double-sided grating samples are shown in figure 5. The experimental results were in good agreement with our theoretical calculations. Two transmission peaks were observed: a strong one around 15 GHz and a weaker peak around 30 GHz. The highest transmission peak was achieved with the asymmetric rectangular grating geometry: 51% at a resonance frequency of 14.5 GHz. The transmission band of this sample was the narrowest among all. 37% and 45% transmission at resonances of 15.6 and 14.6 GHz

Figure 6. Normalized transmission as a function of reception angle. The measurements were made at the resonance frequency of each double-sided grating sample (thin solid curve, sinusoidal grating; dashed curve, symmetric rectangular grating; thick solid curve, asymmetric rectangular grating).

for an air–metal system:

$$\mathbf{k}_{SP} = \mathbf{k}_0 \sin\theta \pm N\mathbf{k}_g \qquad (1)$$

$$k_{SP} = k_0 \sqrt{\frac{\varepsilon_m \varepsilon_0}{\varepsilon_m + \varepsilon_0}} \qquad (2)$$

where $\mathbf{k}_{SP}$, $\mathbf{k}_0$, and $\mathbf{k}_g$ are the wavevectors for SP, incident field, and grating, respectively. ε_m and ε_d denote the permittivity of metallic and dielectric media (air) respectively. In the microwave spectrum, permittivities of metals are very high ($\sim 10^6$) compared to the permittivity of air. Hence, we can safely assume that $k_{SP} \approx k_0$. Since the radiation is normally incident to the grating ($\theta = 0°$), equation (1) becomes $k_{SP} = N k_g$. The coupled SP wavevector k_{SP} should therefore be an integer multiple of $k_g = 2\pi/\lambda_g$. In our samples, λ_g was 16 mm and resonance coupling frequencies were expected to be about $c/\lambda_g = 18.75$ GHz and integer multiples. However, in our experiments and simulations, coupled frequencies shifted towards lower frequencies (~ 15 GHz and integer multiples). This red-shift is due to retardation by the metal. Indeed, this result was in parallel to previously reported EOT measurements. A similar red-shifted SP coupling was reported and explained with a nano-scale metallic grating and subwavelength apertures measured in the optical spectrum [9].

To compare the directivity/beaming property of the samples, transmission data at resonance frequencies were recorded as a function of polar angle. Figure 6 illustrates the normalized transmission intensity as a function of reception angle. All samples featured good beaming properties. The measured transmission sharply decreased with increasing θ. The highest directivity was displayed again by the asymmetric rectangular sample, with an FWHM of 8°. The sinusoidal and symmetric rectangular samples had FWHMs of 9° and 13°, respectively.

The spectral transmission data of the double-sided sinusoidal grating at different reception angles ($\theta = 0°, 10°, 20°,$ and 30°) are shown in figure 7(a). The transmission peak shifted to lower frequencies and the peak intensity decreased with increasing θ. These results implied that at a certain frequency the radiation emerged with maximum intensity at a particular angle from the surface. To

Figure 5. (a) Measured transmission spectrum of the sinusoidal grating sample (thick solid curve) and the reference sample (thin solid curve), and the simulated transmission spectrum (dashed curve). (b) Measured (thick solid curve) and simulated (dashed curve) transmission spectra of the symmetric rectangular grating. (c) Measured (thick solid curve) and simulated (dashed curve) transmission spectra of the symmetric rectangular grating. The inset figures in (a)–(c) show the calculated enhancement factors for the corresponding samples.

were obtained with sinusoidal and symmetric rectangular samples, respectively. In terms of enhancement, all samples displayed higher than 20-fold enhancement at their resonances. An enhancement factor of ~ 25 was achieved with the asymmetric rectangular sample. The simulated transmission spectra presented very similar transmission peaks in terms of resonance frequency and peak intensity.

To compare the measured and simulated results with the analytic SP coupling theory we used the following equations

Table 1. Summary of transmission measurement results.

Sample	SP resonance frequency (GHz)	Peak transmission (%)	Enhancement	FWHM (deg.)
Reference	—	4	—	—
One-sided grating (front-illuminated)	15.1	8	~4	—
One-sided grating (back-illuminated)	16.1	10	~6	8
Double-sided sinusoidal grating	15.6	37	~20	9
Double-sided symmetric rectangular grating	14.6	45	~21	13
Double-sided symmetric rectangular grating	14.5	51	~25	8
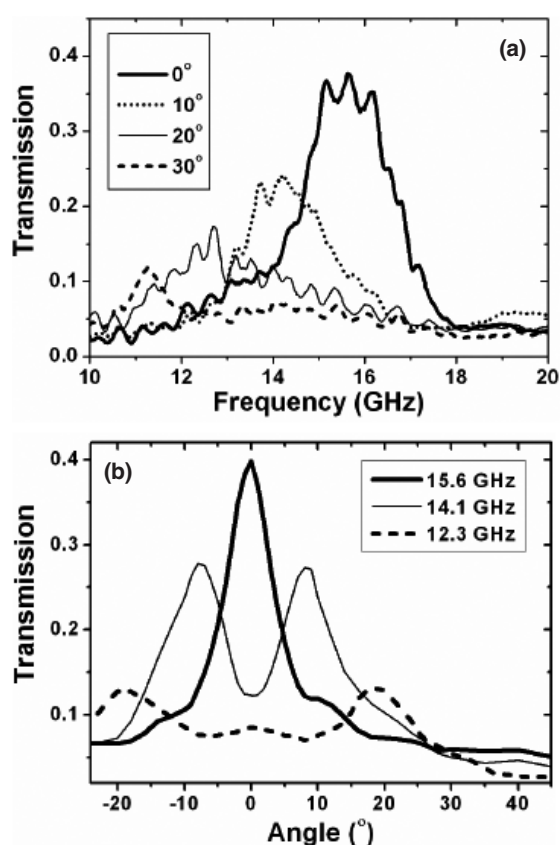
Figure 7. (a) Transmission spectra of double-sided sinusoidal grating sample recorded at various reception angles. (b) Transmission intensity as a function of reception angle at three different frequencies.

period, and m is an integer. A summary of the transmission measurement results is presented in table 1.

4. Conclusion

In conclusion, we have analysed the coupling mechanism between microwave radiation and surface plasmons in 1D metallic grating structures. Enhanced transmission was demonstrated through subwavelength ($\sim\lambda/10$) apertures surrounded by metallic gratings on both surfaces. Several grating geometries were studied in transmission experiments. An experimental enhancement factor as high as 25 and beaming as narrow as 8° FWHM were achieved. Our theoretical simulations were in good agreement with the experimental results.

confirm this statement, transmission intensity as a function of θ was measured at different frequencies. Figure 7(b) presents angular transmission data at 15.6, 14.1, and 12.3 GHz. The corresponding transmission peaks were observed at polar angles of 0°, ±10°, and ±20°, respectively. Theoretical diffraction analysis using the diffraction grating equation,

$$\theta_F^{(m,\pm)}(\lambda) = \sin^{-1}\left(\frac{m\lambda}{d} \pm 1\right) \qquad (3)$$

confirmed our measurement results when the blue-shift due to metal retardation is taken into account. Here, d is the grating

References

[1] Raether H 1988 *Surface Plasmons* (Berlin: Springer)
[2] Teng Y and Stern E A 1967 *Phys. Rev. Lett.* **19** 511–4
[3] Ebbesen T W, Lezec H J, Ghaemi H F, Thio T and Wolf P A 1998 *Nature* **391** 667–9
[4] Porto J A, Garcia-Vidal F J and Pendry J B 1999 *Phys. Rev. Lett.* **83** 2845–8
[5] Schröter U and Heitmann D 1999 *Phys. Rev.* B **58** 15419–21
[6] Takakura Y 2001 *Phys. Rev. Lett.* **86** 5601–3
[7] Barbara A, Quémarais P, Bustarret E and Lopez-Rios T 2002 *Phys. Rev.* B **66** 164103
[8] Steele J M, Moran C E, Lee A, Aguirre C M and Halas N J 2003 *Phys. Rev.* B **68** 205103
[9] Lezec H J, Degiron A, Devaux E, Linke R A, Martin-Moreno L, Garcia-Vidal F J and Ebbesen T W 2002 *Science* **297** 820–2
[10] Martin-Moreno L, Garcia-Vidal F J, Lezec H J, Degiron A and Ebbesen T W 2003 *Phys. Rev. Lett.* **90** 167401
[11] Garcia-Vidal F J, Lezec H J, Ebbesen T W and Martin-Moreno L 2003 *Phys. Rev. Lett.* **90** 213901
[12] Bravo-Abad J, Martin-Moreno L and Garcia-Vidal F J 2004 *Phys. Rev.* E **69** 026601
[13] Grupp D E, Lezec H J, Thio T and Ebbesen T W 1999 *Adv. Mater.* **11** 860–2
[14] Grupp D E, Lezec H J, Thio T, Ebbesen T W, Pellerin K M and Thio T 2000 *Appl. Phys. Lett.* **77** 1569–71
[15] Martin-Moreno L, Garcia-Vidal F J, Lezec H J, Pellerin K M, Thio T, Pendry J B and Ebbesen T W 2001 *Phys. Rev. Lett.* **86** 1114–7
[16] Popov E, Neviere M, Enoch S and Reinisch R 2000 *Phys. Rev.* B **62** 16100–8
[17] Vigoureux J M 2001 *Opt. Commun.* **198** 257–63

[18] Bonod N, Enoch S, Li L, Popov E and Neviere M 2003 *Opt. Express* **11** 482–90

[19] Baida F I, Van Labeke D and Guizal B 2003 *Appl. Opt.* **42** 6811–5

[20] Rivas J G, Schotsch C, Bolivar P H and Kurz H 2003 *Phys. Rev.* B **68** 201306

[21] Hibbins A P, Sambles J R and Lawrence C R 1999 *J. Appl. Phys.* **86** 1791–5

[22] Hibbins A P, Sambles J R and Lawrence C R 2000 *J. Appl. Phys.* **87** 2677–83

[23] Hibbins A P, Sambles J R and Lawrence C R 2002 *Appl. Phys. Lett.* **81** 4661–3

[24] Lockyear M J, Hibbins A P, Sambles J R and Lawrence C R 2004 *Appl. Phys. Lett.* **84** 2040–2

[25] Sigalas M M, Chan C T, Ho K M and Soukoulis C M 1995 *Phys. Rev.* B **52** 11744–51